

Research & Reviews: Journal of Chemistry

Synthesis and Self-Assembly of Some Newly Synthesized Perylene Tetracarboxylic Diimides

D'Cruz ASC and Sankaran KR*

Department of Chemistry, Annamalai University, Annamalainagar, Tamil Nadu, India

Research Article

Received date: 11/04/2016

Accepted date: 08/09/2016

Published date: 13/09/2016

*For Correspondence

Sankaran KR, Department of Chemistry,
Annamalai University, Annamalainagar-608 002,
Tamil Nadu, India, Tel: +919443665919

E-mail: profkrs15@gmail.com

Keywords: PTCDI, SEM, AFM, Phase contrast microscopy, Computational studies

ABSTRACT

Here in this paper, the synthesis of two newly synthesized perylene tetracarboxylic diimides (PTCDIs) namely N,N'-Bis (2,5-diethoxyphenyl) perylene-3,4,9,10-tetracarboxylic diimide and N,N'-Bis (4-butoxyphenyl) perylene-3,4,9,10-tetracarboxylic diimide are reported and are represented as compounds DE-PTCDI and BA-PTCDI respectively. The synthesized compounds were characterized by using different methods such as FT-IR, ^1H NMR, ^{13}C NMR and mass spectral analysis. The scope of this work was to synthesize new PTCDIs and study its optical and morphological properties. The rod like morphological features of both the synthesized compounds were characterized by using various microscopic techniques such as scanning electron microscopy (SEM), optical microscopy, atomic force microscopy (AFM) and phase contrast microscopic techniques. Computational studies too were carried out in order to elucidate the structure of these compounds.

INTRODUCTION

In recent years, many researchers have diverted their focus of interest to the already existing n-type semiconductors as they have been found this area particularly to be quite interesting and challenging to develop for practical use in the organic electronic industry. From all the widely studied n-type materials, perylene tetracarboxylic diimides (PTCDIs) are highly preferred due to its low cost and availability^[1]. Besides this, these compounds are also known to exhibit high molar absorptivity, show high electron affinity, demonstrate excellent photochemical and thermal stabilities, as well as good electrochemical performance^[2,3]. The electrochemical properties exhibited by PTCDIs make them good electron acceptor and electron-transporting materials. They are hence widely used for applications as organic light emitting diodes (OLEDs), organic thin film transistors (OTFTs), solar cells photovoltaic cells, optical switches, lasers, electrophotography, fluorescent light collectors and so forth^[4-7].

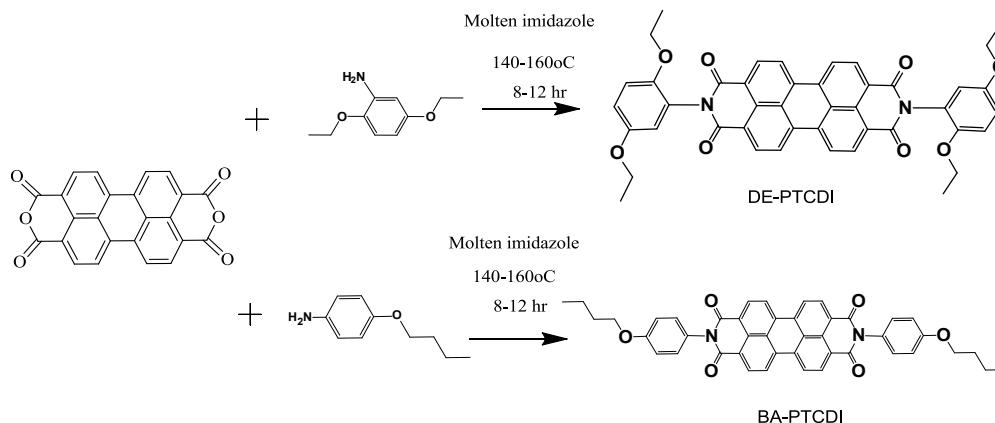
On the other hand, a serious disadvantage with PTCDI lies with its insolubility in a vast major of organic solvents and immobility in air which makes it difficult for organic electronic devices to be operated under ambient conditions. Thus, researchers find this area as a challenging field in the scientific domain and are striving hard to find new routes to develop air stable organic devices. Two methods are used to increase the solubility of PTCDI's. The first method involves substitution at the imide positions using strong electron withdrawing groups or long alkyl chain substituents to obtain the swallow tail conformation whereas, the second method is usually out by substitution at the bay positions of the parent compound. Strong electron withdrawing groups does not only change the redox potentials and the band gap energies of dyes but is also known to influence the semiconducting properties as well as the electron injection barriers into these materials^[8]. Thus, diimides and other such small molecules which contain electron-withdrawing groups show good electron transport properties^[9]. However, fullerenes are a perfect example of a n-type organic semiconductor that does not contain any additional electron withdrawing groups whereas, functionalized fullerenes are found to be suitable candidates for solution-processed n-channel OTFTs^[10,11].

The scope of the work discussed in this paper is the synthesis and characterization of some new PTCDIs and the study of its optical and morphological properties that could help serve as useful applications in the organic electronic industry.

MATERIALS AND METHODS

Materials Used

Perylene-3,4,9,10-tetracarboxylic dianhydride (PTCDA) and imidazole were obtained from Sigma Aldrich, India. Whereas, 2,5-diethoxy aniline and 4-butoxyaniline was purchased from Alfa Aesar, India. All the chemicals were used as such without any further purification (**Scheme 1**).



Scheme 1. N,N'-Bis(2,5-diethoxyphenyl)perylene-3,4,9,10-tetracarboxylic diimide (DE-PTCDI) and N,N'-Bis(4-butoxyphenyl)perylene-3,4,9,10-tetracarboxylic diimide (BA-PTCDI).

Instrumentation

FT-IR measurements from the regions 4000-400 cm^{-1} were performed on a NICOLET AVATAR 360 instrument using KBr pellet. For ^1H NMR and ^{13}C NMR analysis, a small quantity of the synthesized compound was dissolved in approximately 0.5 mL of the desired solvent (CDCl_3) and was recorded on a Bruker 400/100 MHz spectrometer respectively. Chemical shifts were measured in parts per million (ppm). Mass spectral analysis was carried out on a JEOL GCMATE 11 GC Mass spectrometer. SEM image was obtained on a JEOL INDIA Pvt. Ltd., JSM-6610LV instrument. The samples were prepared by casting a drop of the self-assembly solution onto a clean glass slide, followed by annealing it in an oven for about half an hour. The samples were then coated with platinum prior to the SEM measurement. Optical microscopic images were obtained using a MAGNIUS MLX model, MAGNIUS MICROSCOPE, whereas, phase contrast microscopic images were obtained using a NIKON TYPE 120c, NIKON ECLIPSE TS 100 microscope. AFM measurements were performed on an AGILENT -5500 AFM instrument. The images were recorded by non-contact method. Differential scanning calorimetry was performed using NETZSCH STA 449F3 instrument. The samples were recorded upto 350 °C and heated at 5 K min^{-1} in nitrogen.

Experimental

The synthesis of both the compounds was carried out by the condensation reaction of perylene tetracarboxylic dianhydride (PTCDA; 0.395 g, 1 mmol) and 2, 5-diethoxy aniline (0.362 g, 2 mmol)/4-butoxyaniline (0.327 mL, 2 mmol) in the presence of molten imidazole (~6 g) which was taken in a 50 mL round-bottom flask and carried out for a period of 8-12 h at temperatures ranging from 140-160 °C. A nitrogen gas environment was created for the synthesis of compound BA-PTCDI. The completion of the reactions was determined by performing thin layer chromatography. On completion of the reaction, the reaction mixture was then further treated with 100 mL ethanol and 300 mL 2M HCl and was left to stir overnight. The precipitate obtained was washed with copious amount of water until the washings turned neutral. The compound was then dried, weighed and then characterized for further studies.

Whereas, compound BA-PTCDI was treated with 5% HCl washings so as to remove the impurities and was purified by washing the precipitate with copious amount of distilled water till the pH of the washings turned neutral. The purity of the compound was further determined by performing thin layer chromatography using hexane: ethyl acetate (3:2). The raw product was later dried at 100 °C for ~12 h.

DE-PTCDI: ^1H NMR (CDCl_3 , 400 MHz) (ppm): 8.64-8.76 (d, 6H, perylene H), 8.47-8.49 [(d, 1H, perylene H), 6.87-7.0 [(d, 6H, carboxy attached phenyl rings), 3.39-4.05 [(m, 8H, carboxy methylene groups), 1.34-1.42 [(m, 7H, carboxy methyl groups)], 1.12-1.16 [(m, 6H, carboxy methyl groups)], ^{13}C NMR (CDCl_3 , 100 MHz) (ppm): 163.0 (C=O), 123.0-134.5 (perylene C), 114.4 (Ar-C), 64.9 and 64.1 (OCH_2), 14.9 (CH_3), IR (KBr, cm^{-1}): 3114 (Aromatic C-H stretching), 2956-2856 (Aliphatic C-H stretching), 1694 and 1658 (C=O stretching), 1594 (aromatic C=C stretching), 1353 (C-N stretching), MS(EI): m/z calcd, for $\text{C}_{44}\text{H}_{34}\text{N}_2\text{O}_8$, 718.2; Found: 718.7 [M^+]. UV-vis (CHCl_3): λ_{max} (nm) 526, 489, 459; fluorescence (CHCl_3): λ_{max} (nm) 534, 574 ($\lambda_{\text{exc}}=460$ nm); yield: 70%, red powder.

BA-PTCDI: ^1H NMR (400MHz, CDCl_3): δ 8.69-8.77 [(d, 3H, perylene H, (H3)], 7.07-7.09 (d, 2H, H4), 4.03-4.04 (t, 2H, O- CH_2),

2.17 [(s, 3H, H₁)], 1.80-1.84 [(t, 2H, H₂)], 0.90-1.0 (t, 6H, CH₃); IR (KBr, cm⁻¹): ν 3070-2879 (Ar and aliphatic C-H stretching), 1704 and 1661 (C=O stretching), 1589 (aromatic C=C stretching), 1362 (C-N stretching); Mass C₄₄H₃₄N₂O₆: 686.2 (calcd), 686.7 (found); UV-vis (CHCl₃): λ_{\max} (nm) 458, 488, 525; fluorescence (CHCl₃): λ_{\max} (nm) 543, 576 (λ_{exc} = 460 nm); yield: 40%, brown powder.

RESULTS AND DISCUSSION

From **Figure 1**, we can clearly see the well distributed peaks for both of the synthesized compounds DE-PTCDI and BA-PTCDI respectively. For compound DE-PTCDI, carboxy-methyl peaks were observed at 1.12-1.16 and 1.34-1.42 ppm respectively. For compound BA-PTCDI well defined methyl peaks appeared as a triplet at 0.90-1.0 ppm respectively. The detailed ¹H NMR and ¹³C NMR assignments of DE-PTCDI and BA-PTCDI are as mentioned above.

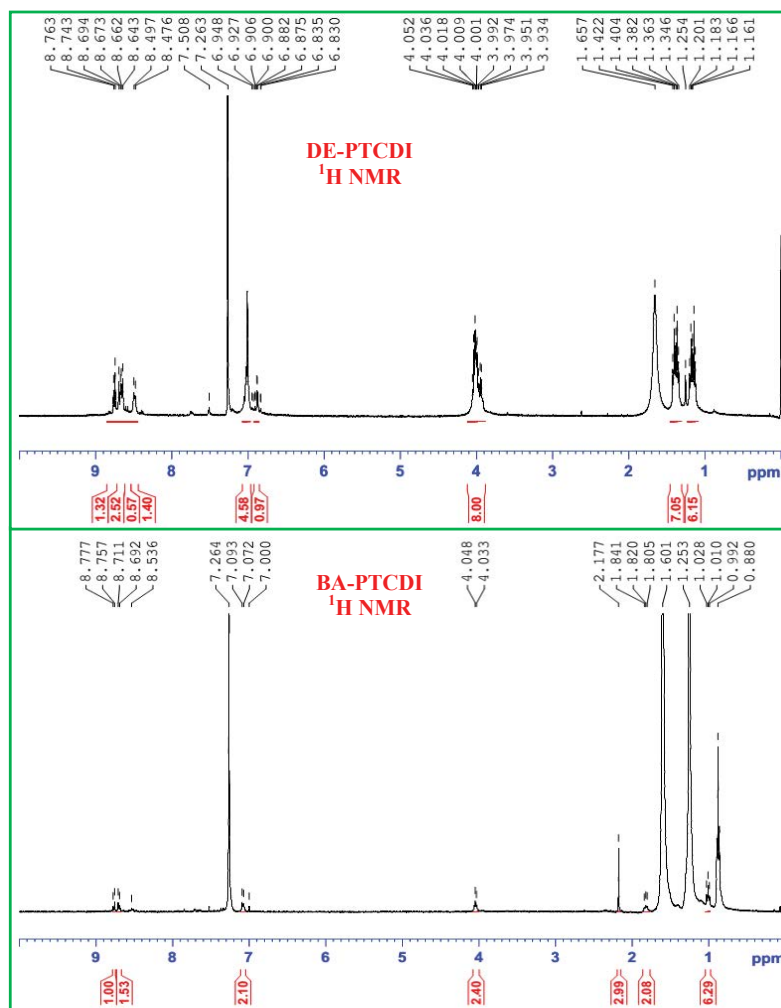


Figure 1. ¹H NMR spectra of (a) DE-PTCDI (b) BA-PTCDI.

Since self-assembly are strongly dependent on the π - π^* interactions and are of prominent importance in the organic electronic industry, a theoretical NMR study at the 3-21 G* level using (Gauge-Including Atomic Orbital) method was carried out in order to have a clear understanding about the measure of the shielding due to the central π -system. The NMR shielding of the synthesized compounds are displayed in **Figure 2**. From **Figure 2**, it can be implied that due to π -stacking interactions, chemical shifts of the perylene protons are highly shielded in NMR as seen from the differentiation in the red and coloured regions.

Optical studies

The solubility of both the synthesized compounds were carried out in various solvents such as chloroform, dichloromethane (DCM), ethanol, methanol, acetonitrile, DMSO, acetone and hexane. The synthesized compounds were found to be soluble in chloroform and DCM solvent due to its branched alkyl side chains.

The UV-Vis absorption spectra of both the synthesized compounds were recorded in chloroform at various concentrations and are shown in **Figure 3**. The vibronic structure of the absorption bands corresponds to π - π^* electronic transition of the perylene chromophore. The UV-Vis absorption spectra showed typical monomeric π - π transition bands with the three pronounced peaks at around 526/525, 489/488 and 459/458 nm for compounds DE-PTCDI and BA-PTCDI respectively. According to Frank-Condon principle, the maximum absorption peak corresponds in an UV-Vis spectrum to vertical excitation [42]. These peaks correspond to the 0-0, 0-1 and 0-2 electronic transitions of perylene diimide core in the monomeric state [43]. There is no shift in λ_{\max} position

with increasing concentration of the compound. In other words, it can be clearly said that the position of the maxima remained unaffected by the change in alkyl chain length of the different substituents incorporated at the imide positions of the perylene moiety. It can be observed that both of the synthesized compounds showed well defined S_0-S_1 absorption band in the visible region, which is a prominent feature of the aromatic perylene core and the dipole moment were directed parallel to the long axis of the molecule ^[14].

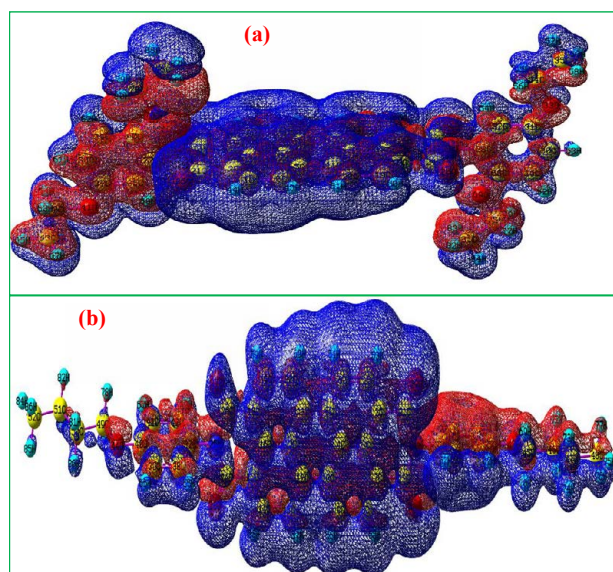


Figure 2. NMR shielding of (a) DE-PTCDI (b) BA-PTCDI.

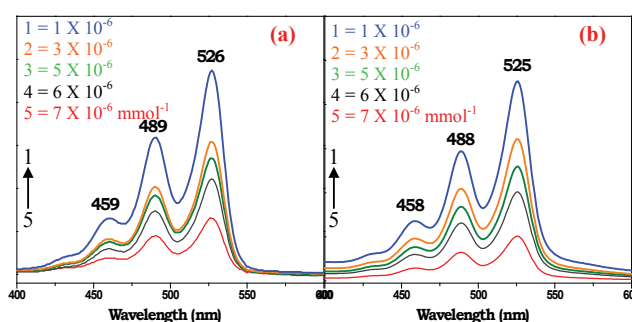


Figure 3. UV-Vis spectra of (a) DE-PTCDI (b) BA-PTCDI.

According to studies carried out by Graser et al. the degree of “area overlap” of successive π -conjugated perylene moieties simply determined the shift of the absorption maximum ^[15,16].

The fluorescence spectra of the synthesized compounds were recorded in chloroform at varying concentrations using excitation at 460 nm. For compound DE-PTCDI, two fine emission peaks appeared at 534 and 574 nm respectively. Whereas, two characteristic emission peaks were observed at around 543 and 576 nm respectively for compound BA-PTCDI. The fluorescence spectra depict the mirror image of the absorption ^[17] due to the position of the two nitrogens at the node in π orbitals ^[8,18]. Both the synthesized compounds showed similar Stokes shift values of ~ 9 -10 nm. This is the same order of magnitude of other perylene diimides as mentioned in literature. Stokes shift in general also depends upon the aggregate size and also on the disorder strength of the compounds. Thus it can be observed that the substitution of the side chains does not change the electronic structure of the PTCDI molecules. The fluorescence spectra of the synthesized compounds are shown in **Figures 4 and 5**.

Self-assembly

The self-assembly of molecules into well-ordered and structured one-dimensional supramolecular architectures is highly dependent on the thermodynamic process and kinetic stability of the compounds ^[19]. Therefore, the self-assembly of the synthesized molecules into 1-D supramolecular structures denote the thermodynamic process ^[20]. In addition, self-assembly of perylene dyes and its derivatives is also largely dependent on the molecular stacking and solubility ^[21]. Thus the choice of solvent used is widely considered for the self-assembly formation. Usually methanol solvent is used due to its weak solvent-molecule interaction which helps enable the formation self-assembly. PTCDI have a strong tendency to form aggregates soon in the chloroform/methanol solution due to its π - π interactions which leads to a diminished fluorescent quantum yield. A slight swirl of the glass vial immediately and upon a short period of time induces supramolecular self-assembly. Such a self-assembly approach takes the advantage of the strong intermolecular π - π interaction, which is enhanced in a solvent where the solvophobic interaction is maximized ^[22].

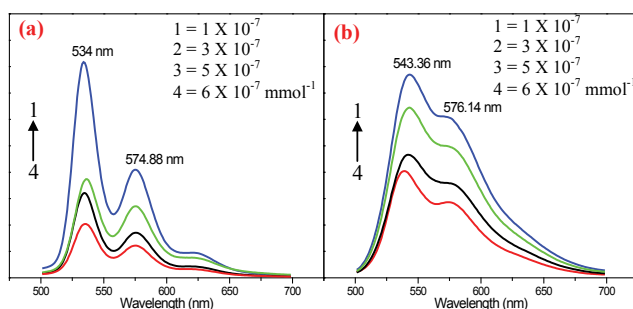


Figure 4. Fluorescence spectra of (a) DE-PTCDI (b) BA-PTCDI.



Figure 5. Self-assembly images of (a) DE-PTCDI (b) BA-PTCDI.

The SEM images of the molecular self-assemblies recorded onto a clean glass slide showed molecular rod like structures for both the synthesized compounds (**Figure 6**). **Figure 7** exhibited rod like morphological feature as seen from optical microscopy. Red emission is particularly well-suited or rather well-known for π -stacked PTCDis and a co-facial perylene compound^[17,23]. These rods like morphological features were found to be similar to the images as shown in **Figure 8**. Strong bright orange molecular rods were observed for compound BA-PTCDI by fluorescence microscopy even for the naked eye as seen in **Figure 9**. The rod shaped morphology of the synthesized compounds was found to be consistent with the distorted π - π stacking, which prevents the molecules from assembling along one dimension^[24].

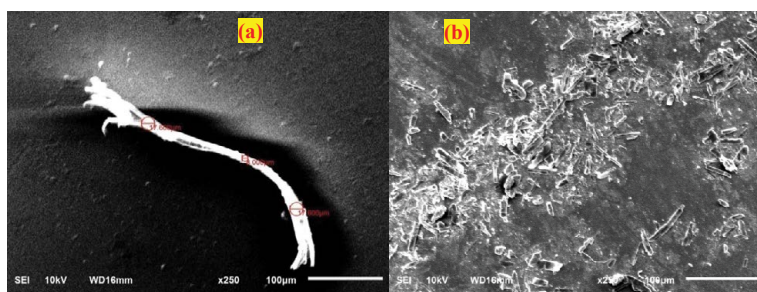


Figure 6. SEM image of (a) DE-PTCDI (b) BA-PTCDI.

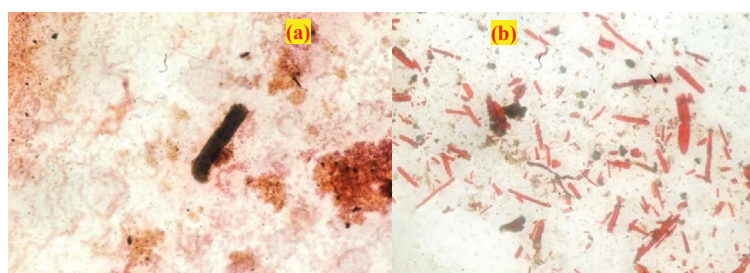


Figure 7. Optical microscopic images of (a) DE-PTCDI (b) BA-PTCDI.

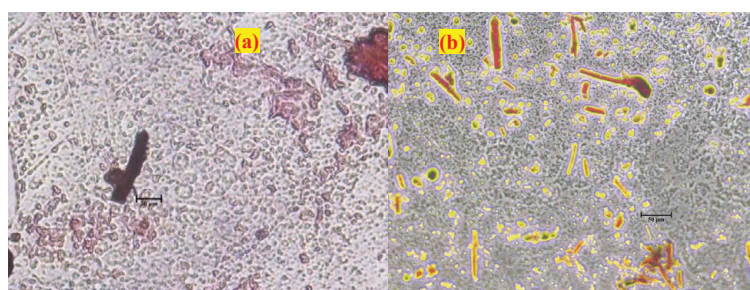


Figure 8. Phase contrast microscopic images of (a) DE-PTCDI (b) BA-PTCDI.

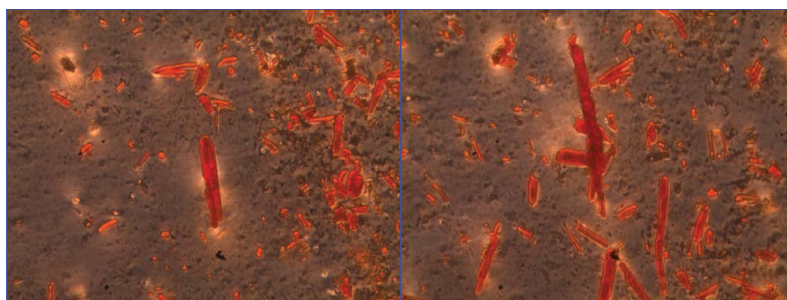
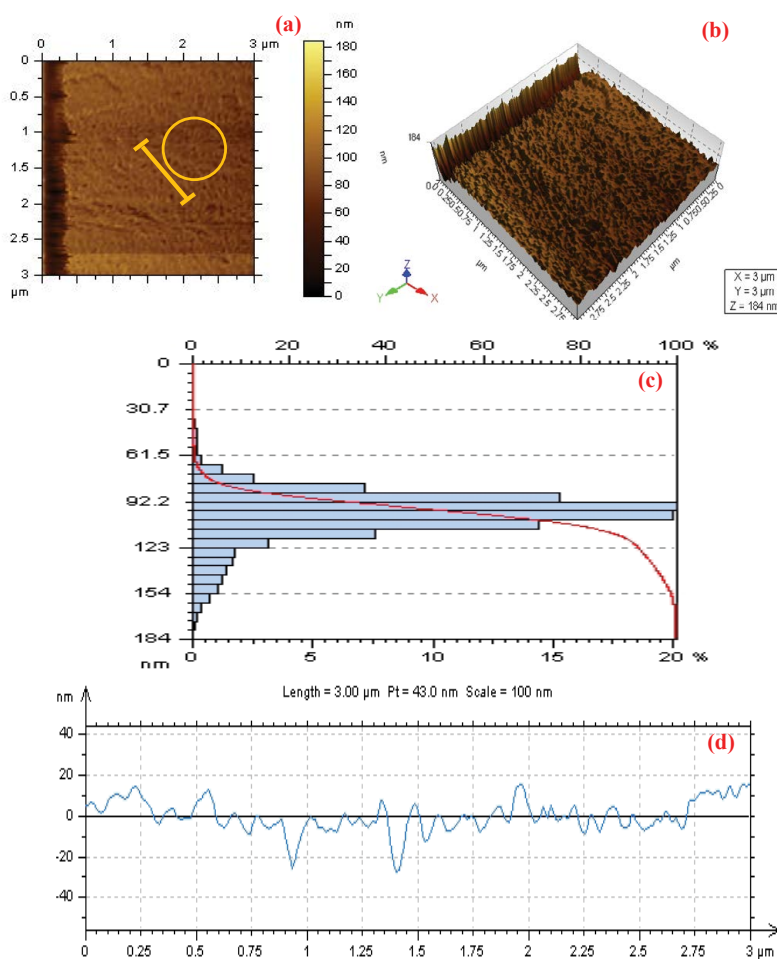


Figure 9. Fluorescence microscopic images of BA-PTCDI.

AFM studies

The morphology of the synthesized compound DE-PTCDI were studied by atomic force microscopy (AFM) using spin coating technique. **Figure 10 (a)** depict a typical AFM image of DE-PTCDI. The corresponding cross-sectional view indicates that the average thickness of DE-PTCDI was found to be approximately about 180 nm. The existence of these small sized particles in compound DE-PTCDI is more clearly reflected in three-dimensional (3D) AFM image **Figure 10 (b)** which showed the wave type projection in the Z direction, which corresponds to uniformly assemble entities of fine grains. Also the formation of large aggregation was found as seen in the **Figures 10 (a) and 10 (b)**. Thus, the above results confirm the micro-texture in the surface of as-synthesized compound DE-PTCDI. The particle size histogram of compound DE-PTCDI is shown in **Figure 10 (c)**. The particle sizes were roughly distributed from 60 to 150 nm. A line is highlighted in **Figure 10 (a)** (two-dimensional (2D) AFM image) and the line profile for the line is shown in **Figure 10 (d)**, and it might reveal rough surface, and particle distribution histogram reveals that the synthesized compound DE-PTCDI shows higher counts at ~250 nm ($1 \text{ nm} = 10^{-9} \text{ m}$).



(a) 2D Atomic force microscopy (AFM) image (height scale 180 nm; scan size, $3 \mu\text{m} \times 3 \mu\text{m}$), (b) 3D AFM image ($2.75 \mu\text{m} \times 2.75 \mu\text{m}$), (c) Particle size distribution of the selected particles (highlighted in Figure 10(a)), (d) Line profile of the selected particles highlighted in Figure 10(a).

Figure 10. Atomic force microscopy image (AFM) of DE-PTCDI by non-contact method.

Thermal studies

Differential scanning calorimetry (DSC) technique was used to study the morphological behaviour of compounds DE-PTCDI

and BA-PTCDI under nitrogen atmosphere (heating rate 5 K min⁻¹). With increasing temperature, four broad endothermic peaks were formed at ~ 100 °C, 220 °C, 250 °C and 310 °C for compound DE-PTCDI respectively. The first three peaks may correspond to various transitions such as crystalline-crystalline or crystalline-isotropic transition while the fourth peak maybe due to the melting point. On the other hand, compound BA-PTCDI showed two endothermic transitions at ~ 70 °C and 340 °C respectively. The first peak may correspond to the crystalline-crystalline transition whereas the second peak maybe due to the melting point. The DSC thermograms are shown in **Figure 11**.

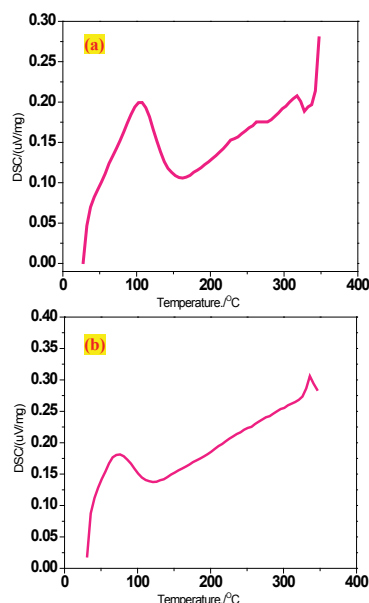


Figure 11. DSC thermograms of (a) DE-PTCDI (b) BA-PTCDI at heating rate of 5 K min⁻¹.

Computational studies

The DFT B3LYP 6-31*G(d,p) basis set is one of the most widely used route to confirm the conformational stability and the molecular geometry of large sized molecules. Optimised molecular structures of the synthesized compounds are graphically visualised in **Figure 12**.

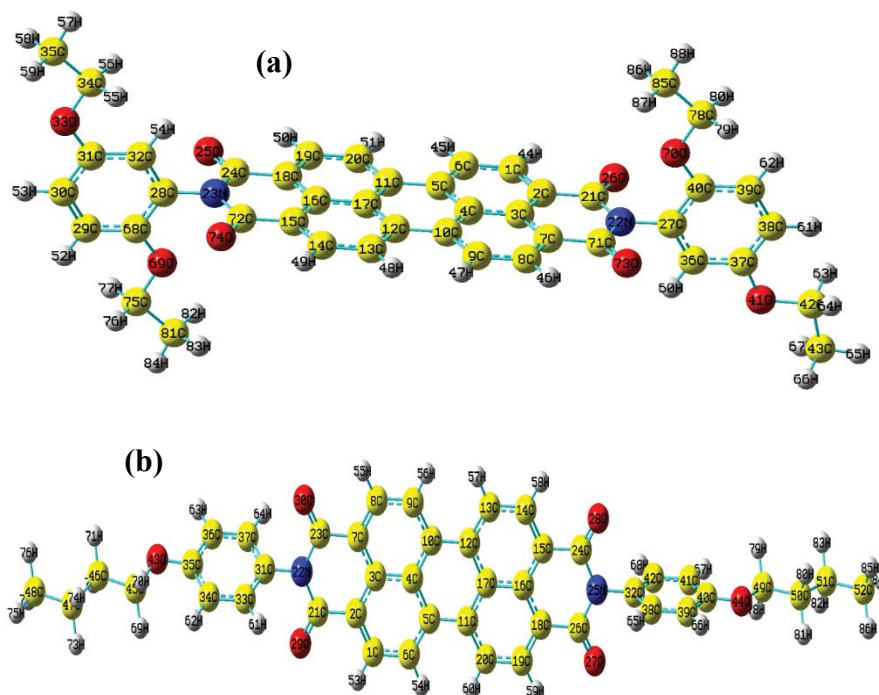


Figure 12. Optimized molecular structures of (a) DE-PTCDI (b) BA-PTCDI.

Frontier molecular orbitals

The frontier molecular orbital (HOMO- LUMO) plays an important role in determining the electrical and optical properties of a compound. HOMO (electron-donating) denotes the highest occupied molecular orbital whereas LUMO (electron-acceptor)

represents the lowest unoccupied molecular orbital. The LUMO exhibits an interesting feature of aromatic diimides which arises as a result of the strong electron-withdrawing power of the imides groups. The large conjugate aromatic ring has strong tendency aggregation via π - π and/or hydrophobic interaction in aqueous solution. PTCDis are known to be good n-type semiconductor materials hence it is easy for them to accept electrons to give anionic radical. Thus PTCDis can be easily reduced in two steps, firstly by generating monoanion radical and secondly by forming a dianion species. Aggregation hence will prevent the reduction from radical anion to dianion because of spin pairing [25].

Also the energy gap play an important role in the design of organic devices. The energy gap is defined as the difference between the ground and first excited state. PTCDis show a direct band gap [26] and are widely used to determine the kinetic stability and chemical reactivity of a compound. This energy gap as calculated from HOMO-LUMO is also useful in determining the molecular electrical transport properties as it is a measure of electron conductivity. Smaller the HOMO-LUMO energy gap, higher is the possibility of charge transfer [27]. In addition, the side-chain substituent groups are also known to alter the conductivity of organic semiconductors. Moreover, introduction of conjugated substituents onto the perylene core are known to interfere or disturb the orbital energy of the perylene π -array which usually leads to a shift of the absorption maximum [28]. Besides this, HOMO and LUMO calculations reveal the charge transfer within the molecule.

The calculated HOMO-LUMO orbital energies are shown in **Figure 13**.

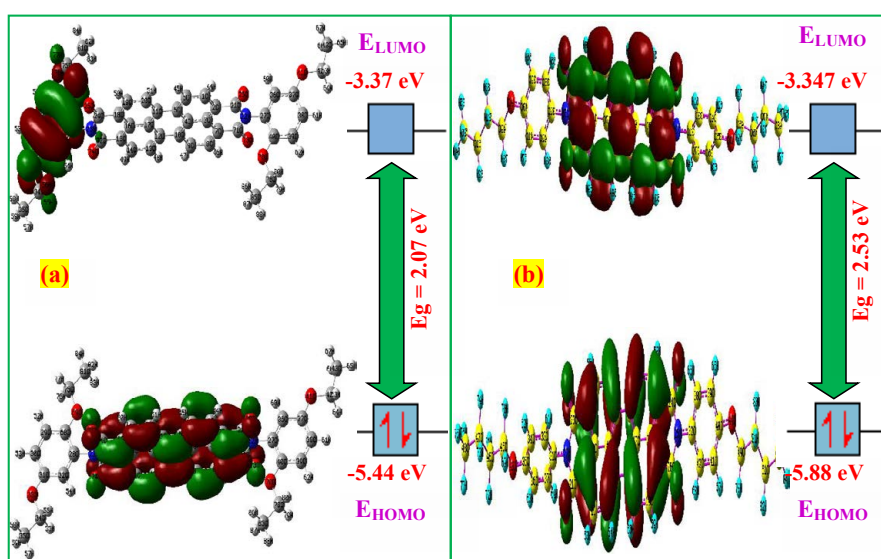


Figure 13. HOMO-LUMO energy gaps of (a) DE-PTCDI (b) BA-PTCDI.

From **Figure 13**, we observe that the perylene (central) π system is the region where the π electrons are delocalized and are influenced by the terminal substituents. This is indicated by the π - π^* transitions. The large band gap values of these synthesized compounds showed that these compounds have strong intermolecular π - π interactions and hence are found suitable to be used in the fabrication and design of new electronic devices.

MEP

MEP is a study of the plot of electrostatic potential mapped onto the constant electron density surface [29]. It serves as a useful tool in determining the reactive sites of a compound. In MEP, the red colour signifies the maximum negative region which is mostly used as an indicator of the electrophilic site, whereas the blue coloured region denotes the area which undergoes nucleophilic attack and hence acts as the positive region [30-32]. Based on its colour grading, MEP reveals important information such as molecular size, shape as well as positive, negative and neutral electrostatic potential regions of the compounds and thus is very beneficial in elucidating molecular structure of the compound along with its physiochemical property relationship [33]. **Figure 14** revealed that the core regions of the central aromatic region is positive as compared to the other regions. The red coloured region contains the oxygen atom and is found to influence the neighbouring atoms with yellow tinges. Besides it also helps to display molecular size and shape for DE-PTCDI and BA-PTCDI respectively.

Mulliken charge transfer

Mulliken atomic charge calculation plays a very significant role in the application of quantum chemical calculations to that of molecular system because of atomic charges effect dipole moment, molecular polarizability, electronic structure and a lot of properties of molecular systems [34]. Mulliken charge transfer helps in providing information regarding the charge distributions over the atoms suggest the formation of donor and acceptor pairs involving the charge transfer in the molecule [35]. **Figure 15** shows the Mulliken charge transfer of compounds DE-PTCDI and BA-PTCDI respectively. From the listed charge values as shown in **Tables 1, S3 and S4**, we observed varying electropositive and electronegative atoms. Electropositive atoms are located at C21,

C71 and C21 for compounds DE-PTCDI and BA-PTCDI respectively. Whereas, electronegative atoms were found to be located at C4 and C8, C14 for compounds DE-PTCDI and BA-PTCDI respectively.

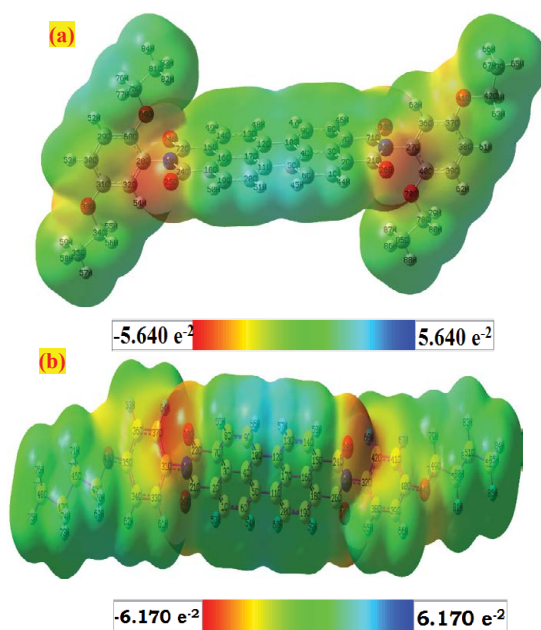


Figure 14. MEP image of (a) DE-PTCDI (b) BA-PTCDI.

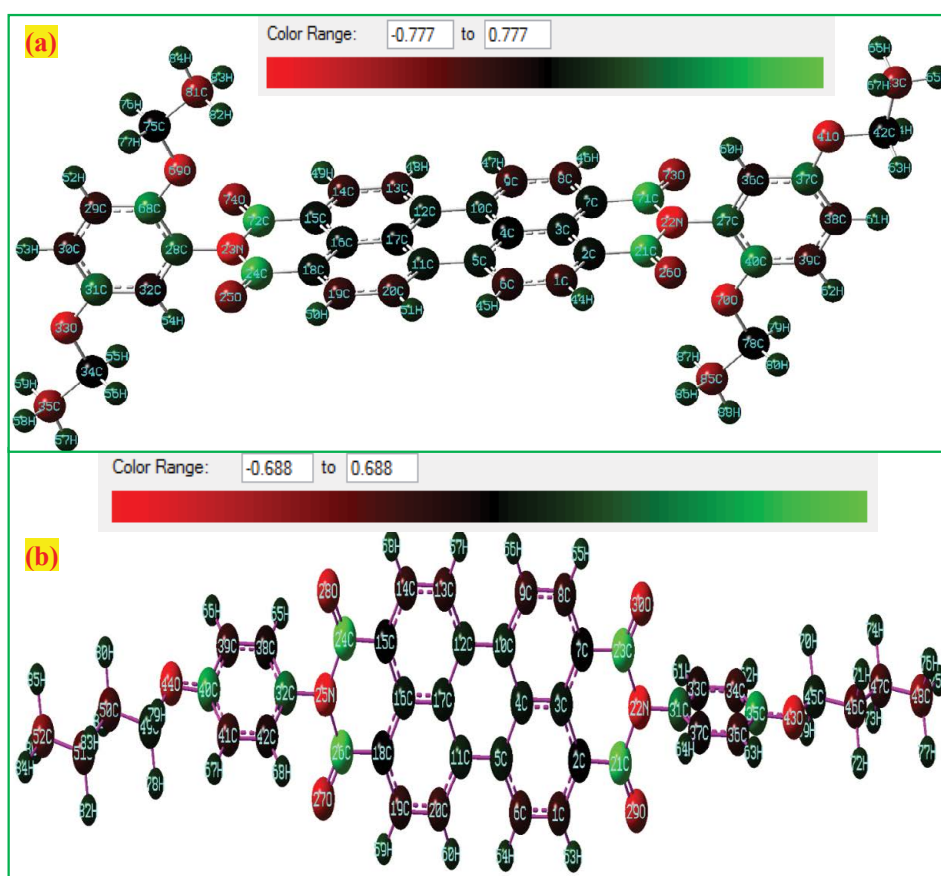


Figure 15. Mulliken charge transfer of (a) DE-PTCDI (b) BA-PTCDI.

Table 1. The calculated HOMO-LUMO orbital energies of compounds DE-PTCDI and BA-PTCDI.

Compound	HOMO	LUMO	E_g
DE-PTCDI	-5.44	-3.37	2.07
BA-PTCDI	-5.88	-3.34	2.53

This indicated that both the synthesized compounds DE-PTCDI and BA-PTCDI showed the presence of both electrophilic and nucleophilic sites. This suggested the presence of intermolecular hydrogen bonding interactions in these compounds.

Natural Bond Orbital (NBO) analysis

NBO analysis is an efficient tool in elucidating the stereo electronic interactions on the reactivity and dynamic behaviour of chemical compounds [35]. NBO helps us analyze the interactions between the intra and intermolecular bonding as well as provides a solid platform for investigating charge transfer or conjugative interactions in molecular system [36]. In NBO analysis, the hyperconjugative $\sigma \rightarrow \sigma^*$ interactions play a very important role. These interactions represent the weak departures from a strictly localized natural Lewis structure that constitutes the primary “non-covalent” effects. In DE-PTCDI In compound 92, the strong intramolecular hyper conjugative interactions of π -electrons are derived as π (C9-C10) to π^* (C7-C8) is 20.70 kJmol⁻¹, π (C16-C18) to π^* (C24-O25) is 22.95 kJmol⁻¹, π (C27-C36) to π^* (C39-C40) is 19.55 kJmol⁻¹, π (C28-C32) to π^* (C29-C68) is 19.51 kJmol⁻¹, π (C29-C68) to π^* (C30-C31) is 20.92 kJmol⁻¹, π (C30-C31) to π^* (C28-C32) is 21.66 kJmol⁻¹, π (C37-C38) to π^* (C27-C36) is 19.43 kJmol⁻¹, π (C21-O26) to π^* (C2-C3) is 115.67 kJmol⁻¹.

In compound BA-PTCDI, the strong intramolecular hyper conjugative interactions of π -electrons are derived as π (C1-C2) to π^* (C3-C7) is 22.24 kJmol⁻¹, π (C3-C7) to π^* (C8-C9) is 22.18 kJmol⁻¹, π (C4-C10) to π^* (C3-C7) is 21.18 kJmol⁻¹, π (C5-C6) to π^* (C1-C2) is 20.45 kJmol⁻¹, π (C8-C9) to π^* (C4-C10) is 22.82 kJmol⁻¹, π (C12-C13) to π^* (C14-C15) is 20.45 kJmol⁻¹, π (C14-C15) to π^* (C24-O28) is 21.68 kJmol⁻¹. Lone pair of electrons available on oxygen atoms O(43) and O(44) is delocalized on the antibonding orbitals of (C34-C35) and (C40-C41) bonds and the delocalization energy is found to be 31.49 kJmol⁻¹.

NBO tables are listed in **Tables S1 and S2 (Supplementary material)**.

CONCLUSIONS

Here in this paper, we have reported the synthesis of two newly synthesized PTCDIs, which were studied for its optical and emission properties. The UV-vis and fluorescence studies recorded in solution state were found to be mirror images of each other. The rod like morphological features observed for the synthesized compounds were found to be consistent with the π - π stacking configuration. Geometrical parameters such as optimized geometry were elucidated to determine the structural property of the synthesized compounds. HOMO-LUMO studies showed that charge transfer does takes place within the molecule. Mulliken charge analysis revealed the confirmation of charge transfer of atoms in the molecule. From the MEP diagrams, the differences between the chemically active and inactive sites were observed which was useful to compare their reactivity of atoms. NBO studies revealed the stability of the molecules arising from hyper-conjugative interaction and charge delocalization. Thus we can conclude that these compounds can be used for suitable applications in the organic electronic industry.

REFERENCES

1. Carmen RDM, et al. Tuning the Charge-Transport Parameters of Perylene Diimide Single Crystals via End and/or Core Functionalization: A Density Functional Theory Investigation. *J Am Chem Soc.* 2010;132:3375-3387.
2. Wenfeng Q, et al. Suzuki Coupling Reaction of 1,6,7,12-Tetrabromoperylene Bisimide. *Org Lett.* 2006;8:867-870.
3. Paramasivan R, et al. Selective Bromination of Perylene Diimides under Mild Conditions. *J Org Chem.* 2007;72:5973-5979.
4. Frank W, et al. Preparation and Characterization of Regioisomerically Pure 1,7-Disubstituted Perylene Bisimide Dyes. *J Org Chem.* 2004;69:7933-7939.
5. Zensheng A, et al. High Electron Mobility in Room-Temperature Discotic Liquid-Crystalline Perylene Diimides. *Adv Mater* 2005;17:2580-2583.
6. Michal W, et al. Self-assembly of perylenediimide based semiconductor on polymer substrate. *Thin Solid Films.* 2010;518:2266-2270.
7. Funda Y, et al. Water-Soluble Green Perylenediimide (PDI) Dyes as Potential Sensitizers for Photodynamic Therapy. *Org Lett.* 2005;7:2885-2887.
8. Langhals. H. Cyclic Carboxylic Imide Structures as Structure Elements of High Stability. *Novel Developments in Perylene Dye Chemistry. Heterocycles.* 1995;40:477-500.
9. Yongfang L. *Organic Optoelectronic Materials.* Springer International Publishing, Switzerland, 2015.
10. Caironi M, et al. *Polymeric and Small-Molecule Semiconductors for Organic Field-Effect Transistors.* Wiley-VCH, Germany, 2015.
11. Schmidt R, et al. High-Performance Air-Stable n-Channel Organic Thin Film Transistors Based on Halogenated Perylene Bisimide Semiconductors. *J Am Chem Soc.* 2009;131:6215-6228.
12. Arivazhagan M and Anitha Rexalin D. Vibrational spectra, UV-vis spectral analysis and HOMO-LUMO studies of 2,4-dichloro-5-nitropyrimidine and 4-methyl-2-(methylthio)pyrimidine. *Spectrochem Acta Part A.* 2013;107:347-358.
13. Wurthner F, et al. A Black Perylene Bisimide Super Gelator with an Unexpected J-Type Absorption Band. *Adv Mater.* 2008;20:1695

14. Thulstrup EW, et al. Polarization spectra in stretched polymer sheets. II. Separation of pi-pi* absorption of symmetrical molecules into components. *J Phys Chem.* 1970;74:3868-3878.
15. Graser F, et al. Perylen-3,4:9,10-bis(dicarboximid)-Pigmenten. *Liebigs Ann Chem.* 1980;12:1994-2011.
16. Klebe G, et al. Crystallochromy as a solid-state effect: correlation of molecular conformation, crystal packing and colour in perylene-3,4:9,10-bis(dicarboximide) pigments. *Acta crystallogr.* 1989;B45:69-77.
17. Liu SG, et al. Self-Organizing Liquid Crystal Perylene Diimide Thin Films: Spectroscopy, Crystallinity, and Molecular Orientation. *J Phys Chem B.* 2002;106:1307-1315.
18. Boobalan G, et al. Synthesis of highly fluorescent and water soluble perylene bisimide. *Chin Chem Lett.* 2012;23:149-153.
19. Okamoto K, et al. Self-Assembly of Optical Molecules with Supramolecular Concepts. *Int J Mol Sci.* 2009;10:1950-1966.
20. Boobalan G, et al. Luminescent one-dimensional nanostructures of perylene bisimides. *Spectrochim Acta Part A.* 2013;113:340-345.
21. Oltean M, et al. Absorption spectra of PTCDI: a combined UV-vis and TD-DFT study, *Spectrochim Acta Part A.* 2012;97:703-710.
22. Boobalan G, et al. Fabrication of luminescent perylene bisimide nanorods. *J Lumin.* 2014;146:387-393.
23. Langhals H and Ismael R. Cyclophanes as Model Compounds for Permanent, Dynamic Aggregates – Induced Chirality with Strong CD Effects. *Eur J Org Chem.* 1998;9:1915-1917.
24. Boobalan G, et al. Self-Assembly, Optical, and Electrical Properties of a Novel Water-Soluble Perylene Bisimide. *J Electron Mater.* 2011;40:2392-2397.
25. Lina Z, et al. Synthesis, Spectra, and Electron-Transfer Reaction of Aspartic Acid-Functionalized Water-Soluble Perylene Bisimide in Aqueous Solution. *Appl Mater Interfaces.* 2013;5:3401-3407.
26. Kis Z, et al. *Synth Met* 2014;194:193–197.
27. Tamer O, et al. Calculations of electronic structure and nonlinear optical parameters of 4-Methoxybenzaldehyde-N-Methyl-4-Stilbazolium Tosylate. *J Appl Spectr.* 2014;80:971.
28. Brian DK, et al. Effect of Substitution on the Optical Properties and HOMO-LUMO Gap of Oligomeric Paraphenylenes. *J Phys Chem A.* 2010;114:13228-13233.
29. Yuhlong OS, et al. Photophysical and Electrochemical Properties of 1,7-Diaryl-Substituted Perylene Diimides. *J Org Chem.* 2005;70:4323–4331.
30. Sarojini K, et al. Synthesis, structural, spectroscopic studies, NBO analysis, NLO and HOMO–LUMO of 4-methyl-N-(3-nitrophenyl) benzene sulfonamide with experimental and theoretical approaches. *Spectrochim Acta Part A.* 2013;108:159-170.
31. Aditya Prasad A and Meenakshisundaram SP. Crystal growth, characterization and Density functional theory computations of supramolecular N-carbamothioyl acetamide. *Cryst Res Technol.* 2015;50:395-404.
32. Prasad AA, et al. Synthesis, crystal growth, characterization and theoretical studies of 4-aminobenzophenonium picrate. *Spectrochim Acta Part A.* 2015;135:46-54.
33. Govindarajan M, et al. Spectroscopic (FT-IR, FT-Raman, UV and NMR) investigation and NLO, HOMO-LUMO, NBO analysis of organic 2,4,5-trichloroaniline. *Spectrochim Acta Part A.* 2012;97:231-245.
34. Ramachandran G, et al. Density functional theory and Ab initio studies of vibrational spectroscopic (FT-IR, FT-Raman and UV) first order hyperpolarizabilities, NBO, HOMO–LUMO and TD-DFT analysis of the 1,2-Dihydropyrazolo (4,3-E) Pyrimidin-4-one. *Solid State Sci.* 2013;16:45-52.
35. John XV and Gobinath E. Experimental and theoretical spectroscopic studies, HOMO-LUMO, NBO and NLMO analysis of 3,5-dibromo-2,6-dimethoxy pyridine. *Spectrochim Acta Part A.* 2012;97:215-222.
36. Sebastian S and Sundaraganesan N. The spectroscopic (FT-IR, FT-IR gas phase, FT-Raman and UV) and NBO analysis of 4-Hydroxypiperidine by density functional method. *Spectrochim Acta Part A.* 2010;75:941-952.